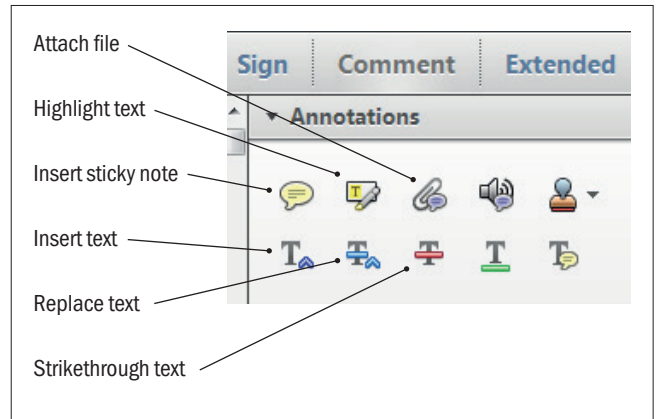# Making corrections to your proof

Please follow these instructions to mark changes or add notes to your proof. Ensure that you have downloaded the most recent version of Acrobat Reader from **https://get.adobe.com** so you have access to the widest range of annotation tools.

The tools you need to use are contained in **Annotations** in the **Comment** toolbar. You can also right-click on the text for several options. The most useful tools have been highlighted here. If you cannot make the desired change with the tools, please insert a sticky note describing the correction.

Please ensure all changes are visible via the 'Comments List' in the annotated PDF so that your corrections are not missed.

| Attach file |
| Highlight text |
| Insert sticky note |
| Insert text |
| Replace text |
| Strikethrough text |

Do not attempt to directly edit the PDF file as changes will not be visible.

Replacing text

To replace text, highlight what you want to change then press the replace text icon, or right-click and press 'Add Note to Replace Text', then insert your text in the pop up box. Highlight the text and right click to style in bold, italic, superscript or subscript.
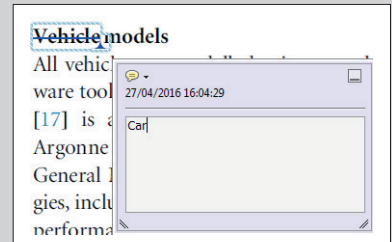
Inserting text

Place your cursor where you want to insert text, then press the insert text icon, or right-click and press 'Insert Text at Cursor', then insert your text in the pop up box. Highlight the text and right click to style in bold, italic, superscript or subscript.
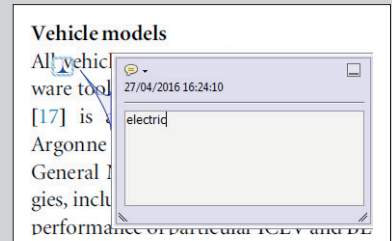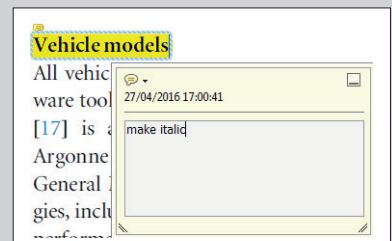
Deleting text

To delete text, highlight what you want to remove then press the strikethrough icon, or right-click and press 'Strikethrough Text'.
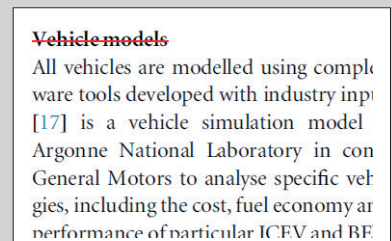
Highlighting text

To highlight text, with the cursor highlight the selected text then press the highlight text icon, or right-click and press 'Highlight text'. If you double click on this highlighted text you can add a comment.

QUERY FORM

The layout of this article has not yet been finalized. This proof may contain columns that are not fully balanced/matched or other typographical imperfections; these issues will be resolved once the final corrections have been incorporated.

Please check that the names of all authors as displayed in the proof are correct. Please check also that all authors are linked correctly to the appropriate affiliations.

If you have an Acknowledgments section, please check that the information there is complete and correct.

Page 10

Q1
Please check the details for any journal references that do not have a link; please update with correct details and supply a CrossRef DOI or NASA ADS link if available.

Page 10

Q2
Please provide the publisher details in references [Batchelor 1953, Frisch 1995, Ruzmaikin et al. 2013, Shalchi 2009].

Page 10

Q3
Please provide the conference location in reference [Jones et al. 1973].

CrossMark

Charged Particle Diffusion in Isotropic Random Magnetic Fields

P. Subedi[1], W. Sonsrettee[2,6], P. Blasi[3,4], D. Ruffolo[2], W. H. Matthaeus[1], D. Montgomery[5], P. Chuychai[1], P. Dmitruk[1,7], M. Wan[1,8],
T. N. Parashar[1], and R. Chhiber[1]
[1] Department of Physics and Astronomy, University of Delaware, Newark, Delaware 19716, USA
[2] Department of Physics, Faculty of Science, Mahidol University, Bangkok 10400, Thailand
[3] INAF/Osservatorio Astrofisico di Arcetri, Largo E. Fermi, 5—I-50125 Firenze, Italy
[4] Gran Sasso Science Institute (INFN), Viale F. Crispi, 7, I-67100 L'Aquila, Italy
[5] Department of Physics and Astronomy, Dartmouth College, Hanover, NH 03755, USA

Abstract

The investigation of the diffusive transport of charged particles in a turbulent magnetic field remains a subject of considerable interest. Research has most frequently concentrated on determining the diffusion coefficient in the presence of a mean magnetic field. Here we consider the diffusion of charged particles in fully three-dimensional isotropic turbulent magnetic fields with no mean field, which may be pertinent to many astrophysical situations. We identify different ranges of particle energy depending upon the ratio of the Larmor radius of the charged particle to the characteristic outer length scale of the turbulence. Two different theoretical models are proposed to calculate the diffusion coefficient, each applicable to a distinct range of particle energies. The theoretical results are compared to those from computer simulations, showing good agreement.

Key words: astroparticle physics – cosmic rays – diffusion – magnetic fields – scattering – turbulence

1. Introduction

Transport of charged particles in many astrophysical systems is governed by the highly turbulent magnetic field, which leads to the diffusion of charged particles in space. Some of the most notable ideas in the study of diffusion of charged particles in magnetic turbulence are quasilinear theory (Jokipii 1966), field line random walk theory (FLRW; e.g., Jokipii & Parker 1968), and nonlinear guiding center theory (Matthaeus et al. 2003). These theories focus on calculating the diffusion of charged particles in directions parallel and perpendicular to a constant mean magnetic field $\boldsymbol{B}_0$, under the influence of a fluctuating magnetic field $\boldsymbol{b}(\boldsymbol{x})$ that depends on position $\boldsymbol{x}$ but not on time. A considerable modification to these theories is required when the fluctuations are isotropic with a zero (or very small) mean field. Such modification turns out to be of the highest importance when describing the transport of cosmic rays (CRs) in the Galaxy, as well as for the modeling of diffusive CR acceleration in astrophysical sources. Here we consider the problem of magnetostatic scattering with $\boldsymbol{B}_0 = 0$, and for fluctuations $\boldsymbol{b}$ that are statistically isotropic, in terms of both polarization and spectral distribution.

The propagation of CRs in the Galaxy is usually modeled as diffusive in a turbulent magnetic field where the rms fluctuations of strength δb are of the same order of magnitude as the large-scale field B_0 (e.g., Jansson & Farrar 2012), $\delta b/B_0 \sim 1$, although it is not clear whether this condition is fulfilled both in the disk and the halo of the Galaxy. On the other hand, supernova shocks, usually invoked to be the main sites of acceleration of Galactic CRs (Blasi 2013), are observed to possess intense turbulent magnetic fields, where the large-scale field, if any, only affects the development of the fast growing instabilities that lead to the existence of intense turbulent fields (Caprioli 2015). At the shock itself, the field is probably well modeled as isotropic with a negligible mean field.

There have been some studies of diffusion of charged particles in magnetic turbulence without a mean field (e.g., Casse et al. 2002; Parizot 2004; de Marco et al. 2007; Plotnikov et al. 2011; Snodin et al. 2016), but a clear theory covering all ranges of particle energies is still lacking. In particular, the simulations carried out by de Marco et al. (2007) clearly showed that, in the limit of large $\delta b/B_0 \gg 1$, the diffusion coefficient of particles with a Larmor radius much smaller than the energy containing scale of the turbulent field closely resembles the one naively estimated from quasilinear theory, which is a rather curious result since such theory applies to the opposite limit. When the field is purely turbulent, the combination of particle diffusion and random walk of magnetic field lines is expected to play a crucial role. Diffusion of magnetic field lines in isotropic turbulence with a zero mean field was examined by Sonsrettee et al. (2015), and that paper is in some ways an antecedent of the present work. We note that the high-energy theory described below was originally presented by David Montgomery.[9]

The transport of charged particles in interplanetary space and the interstellar medium, including in regions of particle acceleration, is highly influenced by the presence of turbulent magnetic fields and their spectral distribution. The nature of particle transport in these fields also depends on particle energy. In general, higher energy particles, with a gyroradius larger than the correlation length of the magnetic field, will sample many uncorrelated field lines within one gyration. Lower energy particles with a gyroradius much smaller than the magnetic field correlation length, on the other hand, will see

---

a relatively coherent large-scale field, and their transport will be heavily affected by resonances with local magnetic fluctuations.

In this paper, we classify the diffusive behavior of charged particles into three different regimes based on the ratio of the Larmor radius R_L of the charged particle to the characteristic outer length scale of turbulence l_c: a high-energy region with $R_L/l_c \gg 1$, an intermediate-energy region with $R_L/l_c \sim 1$, and the low-energy region with $R_L/l_c \ll 1$. Corresponding to the two extreme inequalities, we will develop two corresponding theoretical approaches for particle diffusion in the extreme energy ranges. First, in the high-energy limit, the path of the particle experiences only small deviations from its initial trajectory due to small angle scattering on magnetic field irregularities. In this case, velocity diffusion is achieved when the magnetic fluctuations probed by the particles become uncorrelated. At the opposite extreme, particles with a very small gyroradius will gyrate about the local field produced by the large-scale fluctuations while experiencing perturbations, the most effective of which will be at scales comparable to the gyroradius. This leads to resonant interactions and a random walk of the particle pitch angle. The particle guiding center will eventually reverse direction and parallel spatial diffusion is achieved. The range of validity of both the high-energy and the low-energy asymptotic theories will be extended by building in additional decorrelation effects in the relevant Lagrangian correlation functions, thereby providing an accurate description of the particle mean-free paths also in the intermediate range of energies.

The paper is organized as follows. In Section 2, we write down the fundamental equations describing the diffusive motion of the particles in velocity (or momentum) space. In Section 3, we specialize the theory to the high-energy regime. In Section 4, we show that a nonlinear theory can be developed that reproduces the high-energy behavior of the diffusion coefficient (Section 3) for $R_L/l_c \gg 1$ while also describing the results of numerical simulations down to $R_L/l_c \approx 0.5$. Finally, in Section 5, we describe our formulation of a low-energy theory that, while accounting for particle-wave resonances, also keeps a memory of perpendicular decorrelation, thereby describing simulation results for $R_L/l_c \lesssim 0.5$. A detailed comparison of our theoretically calculated spatial diffusion coefficients with the results of numerical simulations is discussed in Section 6. We summarize in Section 7. Three Appendices are included. The first derives the relationship between velocity diffusion and real space diffusion for isotropic turbulence. The second estimates the angular deflection of a field line over scales in the inertial range and justifies neglecting such deflection in the low-energy theory. The third compares the numerical simulation results with the theories developed in this work when applied to interplanetary parameters.

2. Velocity Space Diffusion and Spatial Diffusion

Since the turbulence is isotropic, and the the particle speed $|v|$ is constant in the absence of electric fields, the velocity space diffusion tensor is expected to have an isotropic form (Batchelor 1953),

$$D_{ij}(v) = (\delta_{ij} - \hat{v}_i \hat{v}_j) D_v, \quad (1)$$

which implies that

$$D_v = \frac{1}{2} Tr[D_{ij}(v)]. \quad (2)$$

The distribution function of test particles obeys the Fokker–Planck equation in velocity space, which when spatial gradients are present can be written as

$$\frac{\partial f}{\partial t} + v \cdot \nabla f = \frac{\partial}{\partial v_i} D_{ij} \frac{\partial f}{\partial v_j}. \quad (3)$$

Plugging in the isotropic form of the velocity space diffusion (Equation (1)) into Equation (3), we get

$$\frac{\partial f}{\partial t} + v \cdot \nabla f = D_v \nabla_\perp^2 f, \quad (4)$$

where $\nabla_\perp^2$ stands for that part of the velocity space Laplacian in spherical co-ordinates that involves no radial derivatives.

To make a connection with spatial diffusion, we construct a multiple timescale solution of Equation (4), by breaking down time and spatial scales into fast (τ, ξ) and slow variables (T, X). We seek a solution with $f = f^{(0)} + \epsilon f^{(1)} + \epsilon^2 f^{(2)} + ...$ where $\epsilon \ll 1$. The qth order distribution function can be expanded in the spherical harmonics as

$$f^{(q)} = \sum_{l,m} C_{lm}^{(q)}(x, v, t) Y_{lm}(\theta, \phi). \quad (5)$$

The details of the multiple timescale solution are given in Appendix A, where a relationship between the velocity space diffusion coefficient D_v and spatial diffusion coefficient κ is obtained:

$$\kappa = \kappa_{xx} = \kappa_{yy} = \kappa_{zz} = \frac{v^4}{6 D_v}. \quad (6)$$

The mean-free path (λ) in terms of the diffusion coefficient is simply

$$\lambda = \frac{3\kappa}{v}. \quad (7)$$

Particle statistics may be related to the spatial diffusion coefficient by the Taylor–Green–Kubo (TGK) formula (Taylor 1922; Green 1951; Kubo 1957):

$$\kappa_{xx} \equiv \lim_{t \to \infty} \frac{\langle \Delta x^2 \rangle}{2t} = \int_0^\infty dt \, \langle v_x(0) v_x(t) \rangle. \quad (8)$$

This formula, with v_x interpreted as the guiding center velocity in the x-direction, was used to calculate the diffusion coefficient in theories that have a mean magnetic field, e.g., BAM theory (Bieber & Matthaeus 1997), the original NLGC theory (Matthaeus et al. 2003), etc.

The velocity space diffusion coefficient can also be written in a TGK formulation as

$$D_{ij}(v) = \int_0^\infty dt \left\langle \frac{dv_i}{dt} \bigg|_0 \frac{dv_j}{dt} \bigg|_t \right\rangle. \quad (9)$$

To calculate the rate of change of velocity in Equation (9), we use the Newton–Lorentz equation of motion

$$\frac{dv}{dt} = \frac{q}{m\gamma c}(v \times b) = \alpha(v \times b), \quad (10)$$

where q and m are the particle charge and mass, respectively, γ is the Lorentz factor, c is the speed of light, $\boldsymbol{b}$ is the magnetic fluctuation field and we define $\alpha = q/(m\gamma c)$. Apply the Newton–Lorentz equation in Equation (9) to find

$$D_{ij}(v) = \alpha^2 \int_0^\infty dt \ \epsilon_{i\alpha\beta}\epsilon_{j\gamma\eta}\langle v_\alpha(0)v_\gamma(t)b_\beta(0)b_\eta[\boldsymbol{x}(t)]\rangle. \tag{11}$$

Assuming that the particle velocity and magnetic field are uncorrelated (as would be the case, e.g., for an isotropic particle distribution) and that the turbulence is statistically homogeneous, one finds

$$D_{ij}(v) = \alpha^2 \epsilon_{i\alpha\beta}\epsilon_{j\gamma\eta}\int_0^\infty dt\,\langle v_\alpha(0)v_\gamma(t)\rangle\langle b_\beta(0)b_\eta[\boldsymbol{x}(t)]\rangle. \tag{12}$$

Equation (1) is used to simplify Equation (12). The high-energy theory and nonlinear theory differ in the treatment of the correlation tensors in Equation (12) (more details are in Sections 3 and 4). Section 5 contains a theoretical description of diffusive transport for low-energy particles.

3. High-energy Theory

Very-high-energy particles with Larmor radii much larger than the correlation scale will experience only minor deflections from their original path because they complete a distance equivalent to the correlation length of the magnetic field. This corresponds to the high-energy theory developed in this section, applicable when $R_L/l_c \gg 1$.

The appropriate simplifying assumptions in this case are that the displacement follows a straight line $\boldsymbol{x}(t) = \boldsymbol{v}t$, and, that the velocity autocorrelation is simply $\langle v_\alpha(0)v_\gamma(t)\rangle = v_\alpha v_\gamma$. Using these, Equation (12) can be written as

$$D_{ij}(v) = \alpha^2 \epsilon_{i\alpha\beta}\epsilon_{j\gamma\eta}v_\alpha v_\gamma \int_0^\infty dt \ \langle b_\beta(0)b_\eta(\boldsymbol{x}(t)=\boldsymbol{v}t)\rangle. \tag{13}$$

In view of Equation (2), computing the trace of Equation (13) gives an expression for the high-energy velocity space diffusion coefficient,

$$D_v = \frac{\alpha^2 v\delta b^2 l_c}{3}, \tag{14}$$

where δb is the rms magnetic field and the correlation length is

$$l_c = \frac{v\int_0^\infty dt\,\langle b_i(0)b_i(vt,0,0)\rangle}{\delta b^2}. \tag{15}$$

Notice that D_v is independent of the spectrum of turbulence because the only thing that matters is the fact that most energy is in magnetic fluctuations at a fixed scale $\sim l_c$ and at that scale we may assume that the effective magnetic field seen by the particle is the rms field δb. Plugging D_v in Equation (6), in terms of gyrofrequency $\Omega_0 = \alpha\delta b$, the spatial diffusion coefficient is then

$$\kappa_{xx} = \kappa_{yy} = \kappa_{zz} = \frac{v^3}{2\Omega_0^2 l_c}. \tag{16}$$

This result is not entirely new to the astrophysics community (see, e.g., Aloisio & Berezinsky 2004), though we give a more formal derivation. An intuitive derivation of Equation (16) proceeds as follows. Suppose that most of the power in the magnetic field spectrum is on a spatial scale l_c, which is much smaller than the Larmor radius of particles. Then one can think of a very large but otherwise arbitrary distance l_d as being tiled with cells of size l_c. In each cell, when $R_L \gg l_c$, one has a deflection of the order $l_c/R_L \ll 1$. The average angle of deflection when there are n scatterings satisfies

$$\langle \theta^2 \rangle = n\left(\frac{l_c}{R_L}\right)^2, \tag{17}$$

where $n = l_d/l_c$. Now, the average deflection angle is of the order of unity when

$$l_d = \frac{R_L^2}{l_c}. \tag{18}$$

At that point the distance is also $l_d \sim vt$ (because the displacement from the unperturbed trajectory is small), and the diffusion coefficient is

$$\kappa = \frac{l_d^2}{2t} = \frac{l_d v}{2} = \frac{R_L^2 v}{2l_c} = \frac{v^3}{2\Omega_0^2 l_c}, \tag{19}$$

which is identical to Equation (16).

4. Nonlinear Extended High-energy Theory

For rigidity decreasing toward unity from large values, the assumption above that the unperturbed particle trajectory is a straight line with constant velocity becomes less accurate. Instead, we assume that the velocity autocorrelation is exponential with a characteristic decorrelation time τ,

$$\langle v_\alpha v_\gamma(t)\rangle = (v^2/3)\delta_{\alpha\gamma}e^{-t/\tau}. \tag{20}$$

However, making use of the TGK formula, Equation (8), one sees that the spatial diffusion coefficient κ_{xx} is related to the timescale τ by

$$\kappa_{xx} = \frac{1}{3}v^2\tau. \tag{21}$$

That is, from Equation (6)

$$\tau = \frac{v^2}{2D_v}. \tag{22}$$

Then, using Equations (2), (12), and (20) one finds that

$$D_v = \frac{1}{2}Tr[D_{ij}(v)] = \alpha^2\int_0^\infty dt\frac{v^2}{3}e^{-t/\tau}\langle b_i(0)b_i[\boldsymbol{x}(t)]\rangle, \tag{23}$$

where there is an implied summation over i. The closure for the Lagrangian correlation in this equation should now be reconsidered. In particular, we question the approximation of a straight-line unperturbed trajectory $\boldsymbol{x}(t) = \boldsymbol{v}t$ that was previously used in the high-energy theory. To allow for the effect of perturbations of this trajectory, $\boldsymbol{x}(t)$ may be treated as a random variable. Following the familiar procedure used in other nonlinear diffusion theories (e.g., Matthaeus et al. 2003), Corrsin's independence hypothesis (Corrsin 1959) is used to write the magnetic correlation in terms of the power spectrum in Fourier space to obtain

$$\langle b_i(0)b_i[\boldsymbol{x}(t)]\rangle = \int d\boldsymbol{k}P_{ii}(\boldsymbol{k})\langle e^{i\boldsymbol{k}\cdot\boldsymbol{x}(t)}\rangle. \tag{24}$$

In order to evaluate the characteristic functional $\langle e^{i\mathbf{k}\cdot\mathbf{x}(t)}\rangle$, we now use the approximation of a Gaussian distribution of displacements, along with the random ballistic decorrelation (RBD) approximation (Ruffolo et al. 2012). The latter was first introduced in describing the magnetic FLRW by Ghilea et al. (2011). Here, the result is

$$\langle e^{i\mathbf{k}\cdot\mathbf{x}(t)}\rangle = \langle e^{ik\mu vt}\rangle_\mu = \frac{1}{2}\int_{-1}^{1} d\mu\, e^{ik\mu vt} = \frac{\sin(kvt)}{kvt}. \quad (25)$$

The random ballistic model is justified since the particles undergo ballistic motion at earlier times before they reach the asymptotic diffusive regime.

With τ given by Equation (22), substituting Equation (25) into Equation (24) and then into Equation (23) gives

$$D_v = \alpha^2 \frac{v^2}{3}\int dk E(k)\int_0^\infty dt \frac{\sin(kvt)}{kvt}e^{-2tD_v/v^2}, \quad (26)$$

where $E(k) = 4\pi k^2 P_{ii}(\mathbf{k})$ is the omnidirectional energy spectrum. If we take the limit $\tau = v^2/(2D_v) \to \infty$ in Equation (26), Equation (14) is recovered, which is the high-energy limit. Hence, the nonlinear theory allows departures from the high-energy limit, but also recovers the exact form of the high-energy limit as τ becomes large. More generally, Equation (26) is an implicit equation for D_v and Equation (6) gives the spatial diffusion coefficient. It is worth pointing out that another standard approximation would be to treat the trajectories of the particles as having a diffusive distribution (DD) for the purpose of calculating the Lagrangian magnetic correlation function (Matthaeus et al. 2003; Bieber et al. 2004; Shalchi 2006, 2010). In that case, the ensemble average on the left-hand side of Equation (25) would then be $\langle e^{i\mathbf{k}\cdot\mathbf{x}(t)}\rangle = e^{-k^2\kappa_{xx}t}$. This alternative approach, however, fails to predict the high-energy behavior of the particles where the particles are ballistic for a long time before undergoing multiple deflections to reach the diffusive limit. For the intermediate range DD converges with the RBD model.

5. Low-energy Quasilinear Theory

Low-energy particles $(R_L/l_c \ll 1)$ behave entirely differently because they experience a local mean magnetic field due to large-scale fluctuations. These small gyroradius particles typically scatter before moving far enough for the local mean field to average to zero. In such circumstances, there are two dominant effects that are expected to contribute to transport and diffusion: FLRW and a kind of resonant wave particle scattering in which the local field acts as a mean field that organizes the particle gyro-motion.

In the presence of FLRW alone, particles would follow magnetic field lines and achieve spatial diffusion as the magnetic field lines diffuse in space. Decorrelation of the particle trajectories due to this mechanism (Jokipii & Parker 1968; Hauff et al. 2010) gives rise to an energy-independent mean-free path. This would not explain the results of our numerical simulations, as discussed below. One may, however, estimate from a simple Kolmogorov turbulence theory the degree to which the field lines bend for distances shorter than a correlation scale, as is done in Appendix B. The conclusion is that the angular deflection of the mean field seen by a particle in moving over a scale l is small provided that l/l_c

is small, i.e., the scale l lies deep in the inertial range. This conclusion is also empirically supported, in that the numerical results (Figure 2) show that at low energy the particle mean-free path is smaller than the correlation length of the magnetic field. For lower energy the local mean field, due to the large-scale parts of the spectrum, becomes increasingly coherent.

Making the assumption that the local mean field remains well defined for a long enough distance, we may examine whether the resonant scattering of particles on fluctuations with wavenumbers around the inverse of the Larmor radius (Jokipii 1966; Fisk et al. 1974) provides effective scattering, in the regime in which turbulence is weak compared to a locally evaluated large-scale mean magnetic field. Of course if the small-scale power is suppressed, then one recovers the FLRW result (see also Karimabadi et al. 1992; Mace et al. 2012).

In the presence of a guide field, the original quasilinear theory (Jokipii 1966) represents the standard tool for calculating resonant pitch angle diffusion coefficients of particles. It is successful in predicting the resonant scattering of the particles in the case of a slab fluctuation field (wave vectors parallel to the mean field) but may require some modification in other fluctuation geometries (e.g., Qin et al. 2002). Nonlinear theories are also useful in attaining better agreement with the results of numerical simulations of particle propagation (Dupree 1966, 1967; Owens 1974; Matthaeus et al. 2003; Shalchi et al. 2004; Shalchi 2006).

In the present case of isotropic turbulence, with no guide field, the assumptions of QLT can no longer be applied, though we are encouraged to proceed based on the above reasoning concerning the local mean field. To be specific, it is useful to first put forward a physical explanation of the approach we propose to describe the low-energy regime: if the power spectrum of magnetic fluctuations is such that most power is on scales of the order of $\sim l_c$, then particles with Larmor radius much smaller than l_c move following a roughly ordered magnetic field line at least until a distance of $\sim l_c$ has been covered. On such scales, the propagation is diffusive in the direction of the local magnetic field, though particles suffer little motion in the direction perpendicular to that of the local field. Let us refer to this parallel diffusion coefficient as $\kappa_\parallel$, though the physical meaning of this quantity should be kept in mind. The effective velocity of particles in the direction of the local field is $v_p \simeq \kappa_\parallel/l_c$. When particles move over many times the coherence scale l_c, their transport in the directions perpendicular to the original local field becomes evident (due to isotropic turbulence) and one can estimate the global diffusion coefficient as

$$\kappa(p) = \frac{1}{3}L_c v_p \simeq \frac{1}{3}L_c \frac{\kappa_\parallel}{L_c} \simeq \frac{1}{3}\kappa_\parallel. \quad (27)$$

In other words, provided the propagation is diffusive on small scales, the global diffusion coefficient on large scales proceeds with a similar diffusion coefficient to that calculated using the local magnetic field as an effective local guide field. The problem is now reduced to calculating the diffusion coefficient experienced by particles along the local magnetic field. This can be done by using a close analogy to the case of QLT.

The parallel spatial diffusion coefficient $\kappa_\parallel$, is calculated using a well-known relationship between $\kappa_\parallel$ and the pitch angle diffusion coefficient $D_{\mu\mu}$ (Jokipii 1966; Hasselmann &

Wibberenz 1970; Earl 1974),

$$\kappa_{\parallel} = \frac{v^2}{8} \int_{-1}^{1} d\mu \, \frac{(1-\mu^2)^2}{D_{\mu\mu}}. \tag{28}$$

The diffusion coefficient along a fixed direction (e.g., the x-direction) is given by

$$\kappa_{xx} = \kappa_{\parallel} \cos^2 \theta + \kappa_{\perp} \sin^2 \theta, \tag{29}$$

where θ is the angle between the magnetic field direction and the x-axis. Since the particles are expected to travel parallel to the local mean field and undergo resonant pitch-angle scattering, which eventually causes a random walk in the parallel direction with little average perpendicular motion, we neglect $\kappa_{\perp}$ in Equation (29) and average over all directions to obtain

$$\kappa_{xx} = \kappa_{yy} = \kappa_{zz} = \kappa_{\parallel}/3, \tag{30}$$

consistent with Equation (27).

Using the TGK formula, the pitch angle diffusion coefficient is given by

$$D_{\mu\mu}(\mu) = \int_0^{\infty} dt \, \langle \dot{\mu}\dot{\mu}' \rangle, \tag{31}$$

where μ is the pitch angle at time $t = 0$ and μ' is the pitch angle at a later time t. Particles are assumed to follow a local field line. The initial direction of the field line can be assumed without loss of generality to be the z-direction and using $v_z = \mu v$, we get

$$D_{\mu\mu}(\mu) = \frac{1}{v^2} \int_0^{\infty} dt \, \langle \dot{v}_z \dot{v}_z' \rangle. \tag{}$$

Using Equation (10), one can write

$$D_{\mu\mu}(\mu) = \frac{\alpha^2}{v^2} \int_0^{\infty} dt \, [\langle v_x v_x' b_y b_y' \rangle + \langle v_y v_y' b_x b_x' \rangle \\ - \langle v_x v_y' b_y b_x' \rangle - \langle v_y v_x' b_x b_y' \rangle]. \tag{32}$$

The Cartesian x and y components of the velocities are given by

$$v_x = v_{\perp} \sin\phi_0 \quad v_y = v_{\perp} \cos\phi_0 \\ v_x' = v_{\perp} \sin(\Omega t + \phi_0) \quad v_y' = v_{\perp} \cos(\Omega t + \phi_0), \tag{33}$$

where $v_{\perp} = v\sqrt{1 - \mu^2}$ is the perpendicular component of the velocity, Ω is the local gyrofrequency, and ϕ_0 is the initial gyrophase of the particle motion. Assuming the product $b_i b_j'$ is independent of ϕ_0, assuming axi-symmetry of magnetic fluctuations along the local mean field ($\langle b_x b_x' \rangle = \langle b_y b_y' \rangle$ and $\langle b_x b_y' \rangle = \langle b_y b_x' \rangle$), using elementary identities and after averaging over the initial gyrophase ϕ_0, Equation (32) reduces to

$$D_{\mu\mu}(\mu) = \frac{\alpha^2 v_{\perp}^2}{v^2} \left[\int_0^{\infty} dt \, \cos(\Omega t) \langle b_y b_y' \rangle \right]. \tag{34}$$

The Lagrangian two-time correlation function $\langle b_y b_y' \rangle = \langle b_y(0,0) b_y(\boldsymbol{x}(t), t) \rangle$ is greatly simplified using the QLT-like assumption that the particles locally follow straight magnetic field lines in the z-direction with constant pitch angle, so that $z = v\mu t$. Using Corrsin's hypothesis (Corrsin 1959), which is exact for slab fluctuations that vary only along z, the Fourier transform of the correlation function $\langle b_y b_y' \rangle$ in terms of the

power spectrum $P_{yy}(\boldsymbol{k})$ becomes

$$\langle b_y b_y' \rangle = \int \int \int dk_x dk_y dk_z P_{yy}(\boldsymbol{k}) e^{ik_z v\mu t} \langle e^{ik_x x} e^{ik_y y} \rangle. \tag{35}$$

In the following two subsections, we proceed to evaluate Equation (35) by adopting different approximations for the characteristic functional $\langle e^{ik_x x} e^{ik_y y} \rangle$ that describes the statistics of the local random perpendicular displacements $x(t)$ and $y(t)$.

5.1. Standard QLT Approach

When the perpendicular displacements $x(t)$, $y(t)$ are very small, we may adopt the approximation $\langle e^{ik_x x} e^{ik_y y} \rangle \approx 1$. This can be viewed as an approximation that the particle is at its guiding center, or that the fluctuations b_x and b_y are independent of x and y. This approximation is implemented in standard QLT, and is exact in one-dimensional slab geometry (Jokipii 1966). Using this in Equation (35), one finds

$$\langle b_y b_y' \rangle = \int dk_z \left[\int \int dk_x dk_y P_{yy}(\boldsymbol{k}) \right] e^{ik_z v\mu t}. \tag{36}$$

In the usual way, we define $E_y(k_z) = \int \int P_{yy}(\boldsymbol{k}) dk_x dk_y$ as a one-dimensional reduced transverse spectrum function. Substituting Equation (36) in Equation (34), and carrying out the time integral yields a Dirac delta function that defines the resonance. Then, the integral over the parallel wave number (k_z) gives

$$D_{\mu\mu} = \frac{\pi\alpha^2(1-\mu^2)}{v} \left[\frac{E_y\left(k_z = \frac{\Omega}{v|\mu|}\right)}{|\mu|} \right], \tag{37}$$

which is the standard QLT result.

One modification applicable to isotropic turbulence that we would like to discuss in detail is related to the μ dependence of $D_{\mu\mu}$ in Equation (37). It is well known that quasilinear theory does not provide correct pitch angle diffusion coefficients for pitch angles close to $90°$ ($\mu \approx 0$) where nonlinear effects are important (Bieber et al. 1988; Tautz et al. 2008; Shalchi 2009, p. 362). This problem was discovered in the years after quasilinear theory had been proposed (Jones et al. 1973; Owens 1974; Goldstein 1976). The strict quasilinear calculation using Equation (37) (for typical spectra of turbulence) has $D_{\mu\mu} \to 0$ as $\mu \to 0$, which is applicable in slab turbulence (Qin & Shalchi 2009) where nonlinear effects are weak. In most other geometries, however, for any realistic finite amplitude fluctuations, nonlinear orbit effects (Karimabadi et al. 1992) allow particles to scatter more easily through the neighborhood of $\mu = 0$ than would be expected from QLT calculations (see also Qin & Shalchi 2009). Our numerical results also indicate that the quasilinear theory for isotropic turbulence as derived using Equations (28), (30), and (37) gives mean-free paths much larger than those obtained from a numerical simulation, since the parallel diffusion coefficient is unrealistically amplified by $D_{\mu\mu}$ near zero in the denominator.

To account for such nonlinear effects, we consider an ansatz that the pitch angle dependence of $D_{\mu\mu}$ is of the form $D_{\mu\mu} \propto 1 - \mu^2$ and set $|\mu| = 1$ inside the square bracket of Equation (37) so that $D_{\mu\mu}$ has a finite nonzero value at $\mu = 0$. Before implementing this, we checked our numerical simulation results for the pitch angle distribution. For $D_{\mu\mu} \propto 1 - \mu^2$ (isotropic scattering), the eigenfunctions of the diffusion

operator are Legendre polynomials, and at late times when the pitch angle distribution is nearly isotropic, the distribution should be dominated by the most slowly evolving eigenfunctions, $P_0 = 1$ and $P_1 = \mu$, yielding a nearly linear pitch-angle distribution. We indeed found this in our simulation data. Thus we implemented the ansatz, which is more appropriate for our case of isotropic turbulence with $B_0 = 0$ than for a perturbative situation with $b \ll B_0$, where nonlinear effects are weak. The ansatz is also justified a posteriori in Section 6, where the theoretical predictions now provide a much better fit to the numerical results.

With this physically motivated modification, the simplified pitch-angle diffusion coefficient can be written as

$$D_{\mu\mu} = \frac{\pi \alpha^2 (1 - \mu^2)}{v} E_z \left(k_z = \frac{\Omega}{v} \right). \tag{38}$$

If we assume that the local mean field is constant throughout the system with magnitude B_{local}, then in Kolmogorov turbulence $E_z \sim k_z^{-5/3}$ and (from Equation (10)) $\alpha = \Omega/B_{\text{local}}$ with $\Omega = v/R_L$, it is straightforward to show that the substitution of Equation (38) into (28) gives $\kappa \sim v l_c (R_L/l_c)^{1/3}$ and the mean-free path (Equation (7)) scales as $\lambda \sim l_c (R_L/l_c)^{1/3}$.

A further correction that we apply here is related to the variability of the magnetic field strength in an isotropic random field. In the realization of turbulence used here, the components of the magnetic field have a Gaussian distribution (this is also usually a reasonable approximation for fully developed turbulence). Therefore, the gyrofrequency $\Omega = qb/(\gamma mc) = \alpha b$ and Larmor radius $R_L = \gamma mvc/(qb) = v/(\alpha b)$ vary in space as the magnetic field strength b changes. In fact, b is likely to undergo major changes during the parallel scattering process described by $\kappa_{||}$. It is fairly simple to show that b has a Maxwellian distribution given by

$$\mathcal{F}(b) db = 3^{3/2} \sqrt{\frac{2}{\pi}} \frac{b^2}{\delta b^3} e^{-\frac{3b^2}{2\delta b^2}} db, \tag{39}$$

where δb is the root-mean-square field strength. With the above Maxwellian distribution, we use Equation (38) to compute the average $\overline{D_{\mu\mu}(\mu)}$ over the local field b before substitution in Equation (28) to obtain

$$\kappa_{||} = \frac{v^2}{8} \int_{-1}^{1} d\mu \frac{(1 - \mu^2)^2}{\overline{D_{\mu\mu}}}. \tag{40}$$

Equation (30) gives the spatial diffusion coefficient along a particular axis. The mean-free path scaling of $\lambda \sim l_c (R_L/l_c)^{1/3}$ is also maintained.

5.2. Extended Low-energy Theory

As an extension to the above quasilinear approach, we now take into account the perpendicular displacements that enter into consideration in Equation (35). Assuming a Gaussian distribution of the perpendicular displacements x and y implies that

$$\langle e^{ik_x x} e^{ik_y y} \rangle = e^{-\frac{1}{2}[\langle x^2 \rangle k_x^2 + \langle y^2 \rangle k_y^2]}. \tag{41}$$

Since we are assuming locally an unperturbed orbit about a well-defined local mean magnetic field, it is clear that $\langle x^2 \rangle = \langle y^2 \rangle \sim R_L^2$. In particular, for pitch angle θ and

gyrophase ϕ,

$$x = R_L \sin\theta \cos\phi, \quad y = R_L \sin\theta \sin\phi. \tag{42}$$

After omnidirectional averaging of x^2 and y^2 over θ and ϕ, Equation (41) can be written as

$$\langle e^{ik_x x} e^{ik_y y} \rangle = e^{-k_\perp^2 R_L^2/6}, \tag{43}$$

where $k_\perp^2 = k_x^2 + k_y^2$. This statistical description of the perpendicular displacement is consistent with our earlier assumption that $b_i b_j'$ is independent of the initial gyrophase. Using Equation (34) along with Equations (35) and (43), one finds

$$D_{\mu\mu}(\mu) = \frac{2\pi^2 \alpha^2 (1 - \mu^2)}{v}$$
$$\times \int_0^\infty k_\perp dk_\perp \left[\frac{P_{yy} \left(k_\perp, k_z = \frac{\Omega}{v|\mu|} \right)}{|\mu|} \right] e^{-k_\perp^2 R_L^2/6}. \tag{44}$$

According to the arguments used in Section 5.1, we take into account the presence of nonlinear orbit effects near a $90°$ pitch angle and modify the pitch angle dependence so that $D_{\mu\mu} \sim (1 - \mu^2)$ and set $|\mu| = 1$ inside the square bracket of Equation (44). For the extended case, the pitch angle diffusion coefficient is now given by

$$D_{\mu\mu}(\mu) = \frac{2\pi^2 \alpha^2 (1 - \mu^2)}{v}$$
$$\times \int_0^\infty k_\perp dk_\perp P_{yy} \left(k_\perp, k_z = \frac{\Omega}{v} \right) e^{-k_\perp^2 R_L^2/6}. \tag{45}$$

Note that when the exponential term is set to unity (e.g., for $R_L \to 0$), this reduces to Equation (38). As described in Section 5.1, we average Equation (45) over a Maxwellian distribution of the magnetic field magnitude b before substitution in Equation (28) to obtain our final result for the spatial diffusion coefficient.

The exponential term can be seen as another modification to the original quasilinear theory appropriate for the pitch angle diffusion of low-energy particles in isotropic turbulence. Hence, we use this extended low-energy theory in the following Section 6 to compare with numerical simulation results.

6. Comparison the with Numerical Simulation

In this section, we present results of numerical simulations of charged particle propagation in synthetic magnetostatic turbulence with a specified spectrum. The numerical results are compared to the theoretical formulations described above.

The numerical simulations make use of a homogeneous and isotropic magnetic fluctuation field, generated on a spatial grid with a specified energy spectrum. Trajectories of 2000 particles are obtained by numerical solution of the Newton–Lorentz equation, using a fifth-order Runge–Kutta method with adaptive time-stepping. To satisfy the magnetostatic assumption, the velocity v of the particles is chosen so that $v \gg v_A$, where v_A is the Alfvén speed. The electric field is ignored because it is of the order of $v_A B/c$, where B is the magnetic field and c is the speed of light.
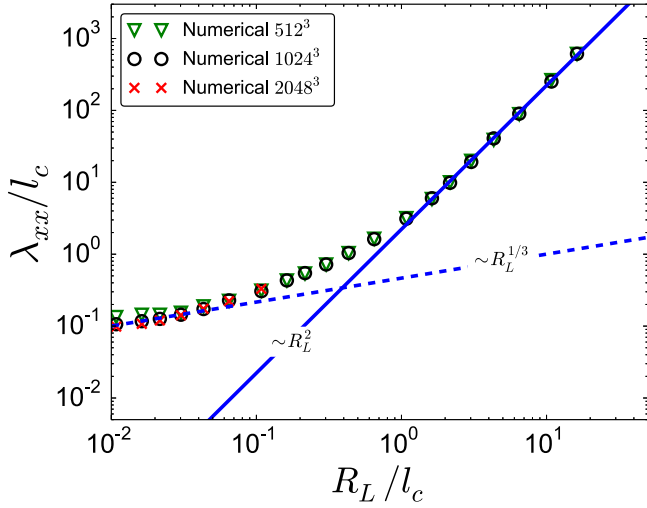
Figure 1. Mean-free path of protons as a function of R_L/l_c (gyroradius divided by correlation scale). The solid line is the high-energy scaling $\lambda_{xx} \sim R_L^2$ and the dashed line is the low-energy scaling $\lambda_{xx} \sim R_L^{1/3}$. The inverted triangles are the results of the 512^3 numerical simulation, circles are those of the 1024^3 simulation, and the crosses are the results of the 2048^3 numerical simulation.

Figure 2. Theoretical vs. numerical results for cosmic rays in isotropic turbulence with a zero mean field, showing good agreement. The circles represent the numerical results, the solid line represents the high-energy theory, the dashed line is the nonlinear theory and the dotted–dashed line is the theoretical estimate for low energies. The energy ranges are shown for cosmic rays in our Galaxy.

The random magnetic field realization is generated in a periodic box as described by Sonsrettee et al. (2015). The functional form of the omnidirectional spectrum used in the numerical simulation is given by

$$E(k) = C\lambda_c \frac{(k\lambda_c)^4}{[1 + (k\lambda_c)^2]^{17/6}},$$

with a normalization constant C, which is used to control the magnetic field strength b. The parameter λ_c is the bendover scale, which is of the same order as the correlation length. This form of $E(k)$ is chosen so that $E(k) \propto k^4$ for low k to be consistent with strict homogeneity (Batchelor 1969), and $E(k) \propto k^{-5/3}$ for high k to represent Kolmogorov scaling in an inertial range of turbulence. We have chosen the Kolmogorov spectrum because is often assumed in scattering theory (Harari et al. 2002; Parizot 2004), but emphasize that the theoretical approach can be applied to any reasonable spectrum.

The diffusion coefficient is calculated from the asymptotic rate of increase of the mean square displacement of the particles

$$\kappa_{xx} = \lim_{t \to \infty} \frac{\langle \Delta x^2 \rangle}{2\Delta t}. \tag{46}$$

The results of the numerical simulations are shown in Figure 1. The general asymptotic trends for the mean-free path at low energies ($R_L \ll l_c$) and high energies ($R_L \gg l_c$) are easy to identify. In the low-energy regime, the mean-free path scales as $\lambda_{xx} \propto R_L^{1/3}$, while in the high-energy regime $\lambda_{xx} \propto R_L^2$, and these scalings are valid whether the particles are relativistic or non-relativistic. As discussed above, this high-energy scaling is obtained irrespective of the power spectrum, provided most power is concentrated on scales around $\sim l_c$. These results confirm previous functional forms proposed by Aloisio & Berezinsky (2004) and Parizot (2004) and the numerical results of Casse et al. (2002), de Marco et al. (2007), and Snodin et al. (2016). Observations of isotopic composition (Obermeier et al. 2012; Aguilar et al. 2016) also support a scaling of $\lambda_{xx} \propto R_L^{1/3}$ at $R_L \ll l_c$.
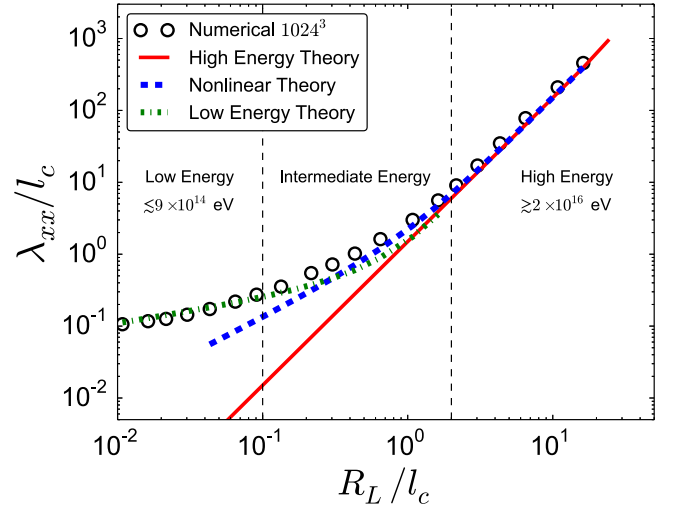
The resonant nature of particle scattering in the low-energy regime makes the numerical simulation rather challenging, in that the resulting mean-free path is sensetive to the resolution in real space, which is equivalent to the number of independent degrees of freedom in k-space used to represent the magnetic power spectrum (see also Snodin et al. 2016). In Figure 1, we show the results of our simulations for 512^3, 1024^3, and 2048^3 real space grid points, from which it is possible to see that the lower resolution (512^3) case does not correctly match the scaling of the mean-free path with Larmor radius. This is because the 512^3 simulation does not numerically resolve the resonant scales corresponding to the Larmor radius of the particles. On the other hand, no appreciable difference can be seen in the two higher resolution cases with 1024^3 and 2048^3 simulations. Hence, we will use the 1024^3 realization for a subsequent discussion of the results.

The mean-free path calculated using the theoretical framework developed above is compared to the results of simulations in Figure 2. These results may be considered as representative of propagation of very-high-energy CR protons in the Galactic magnetic field (Ruzmaikin et al. 2013) with a correlation length of $l_c = 10$ pc and a root-mean-square magnetic field of $\delta b = 0.1$ nT. The Larmor radius of the particles equals the correlation length of the magnetic field fluctuations at energy $E \sim 9 \times 10^{15}$ eV, somewhat above the knee in the all-particle spectrum of Galactic CRs. However, we note that when plotted this way, as mean-free path versus Larmor radius, with both quantities normalized to the correlation scale of the turbulence, the actual curves are identical for any energy range. In Appendix C, we provide a short account of the results of our analysis when applied to non-relativistic and moderately relativistic particles in isotropic turbulence that has parameters akin to heliospheric parameters.

7. Discussion and Conclusions

The spatial diffusion of charged particles in the presence of turbulent magnetic fields is significant in describing the

transport of charged particles in the interplanetary, interstellar, and intergalactic media. Most of the standard descriptions of diffusion involve the existence of a non-negligible ordered field. In this paper, we considered the case of a vanishingly small background ordered magnetic field and studied the diffusive transport of charged particles in isotropic magnetic field (magnetostatic) turbulence. The turbulent Galactic magnetic field, where the mean magnetic field is of the order of fluctuations, is found to have reversals in the field orientation implying the existence of regions with negligible regular fields (Minter & Spangler 1996). Similarly the extragalactic voids might have negligible regular fields (Kronberg 1994; Blasi et al. 1999). In the highly turbulent plasma near supernova shocks that are actively accelerating CRs (Blasi 2013) there may be regions in which the fluctuations might be so large that the present fully isotropic model is applicable. The isotropic assumption is also relevant in other highly disturbed and turbulent plasmas, such as planetary wakes (Gombosi et al. 1979).

Naturally, in the Galactic system, the turbulent magnetic field is not the only complication that appears in a realistic scenario of CR transport. The complex composition of background plasma and the presence of neutral hydrogen atoms that suppress the propagation of waves through ion-neutral damping are examples of factors that could influence the charged particle propagation. Including these complexities in our theoretical calculations is beyond the scope of the current paper. Here we have developed a systematic derivation of charged particle diffusion in the presence of an isotropic turbulent magnetic field and tested its validity using a Monte-Carlo simulation of particles in a synthetically generated turbulent magnetic field. In fact, we would like to point out that incorporating the several factors mentioned above will probably require MHD, hybrid, or PIC simulations that provide a self-consistent picture of the development of the CR transport phenomenon (e.g., Reville et al. 2008; Caprioli & Spitkovsky 2014).

The transport of charged particles in a magnetic field is conceptually simple, requiring mostly the integration of particle trajectories using the Lorentz force (Equation (10)). The detailed treatment is complex, influenced by several parameters like the particle energy, correlation length of turbulence, the geometry of fluctuations, the presence of a dissipation range, and the magnetic Reynolds number. In particular, the study of transport of particles in isotropic magnetic field turbulence is found to be complicated by the different conditions seen by charged particles at high, low, and intermediate energies as defined. Here the controlling parameter is the rigidity, or the ratio of Larmor radius (R_L) to the turbulence correlation length (l_c). When the ratio R_L/l_c is much smaller than one, we refer to the low-energy limit, when it is greater than one, this is the high-energy limit and in between low and high energy lies the intermediate-energy region. We have devised two different theoretical models in an attempt to understand the transport processes in these three regions. Rather than just using parametric and scaling arguments, we provide systematic and thorough theoretical constructs to describe the diffusive transport of particles in each range of energy.

The paths of the higher energy particles are almost straight up to the correlation length of the magnetic field, where the particles undergo only a slight change from the original trajectory. In contrast, the lower energy particles are almost strictly tied to their initial field lines and are pitch-angle scattered due to resonance with small-scale irregularities of the field line. The intermediate-energy particles have a more complicated nonlinear diffusion that connects the two extremes.

The theoretical ideas presented here have been tested against results of detailed numerical experiments using Monte-Carlo simulations of particle propagation in stochastic magnetic fields. The magnetic field constructed for numerical purposes has three-dimensional isotropic fluctuations with a standard Kolmogorov spectrum and no mean field. Diffusion coefficients are calculated using the microscopic displacements of particles along the trajectory. The diffusion coefficients obtained using our numerical simulation are compared to theoretical predictions yielding very good agreement.

Referring again to Figure 2, we can see that both the asymptotic low- and high-energy limits are fitted well by our theoretical approach. The high-energy theory fails in the intermediate- and low-energy regime because the particle velocity changes over a shorter period of time, contrary to the high-energy assumption. The extended low-energy theory compares well with the numerical data even in the intermediate-energy regime when $R_L/l_c \lesssim 0.5$. However, it fails when $R_L/l_c \gtrsim 0.5$ as a consequence of the fact that the effective guide field becomes ill-defined. The nonlinear theory best describes the scattering of the intermediate-energy particles in the range of $R_L/l_c \gtrsim 0.5$. The two extended theories give equal results at $R_L/l_c \approx 0.3$ where they each differ from the numerical results by about 30%.

In summary, we have devised theoretical descriptions of charged particles in isotropic turbulence with no mean field that are applicable to distinct ranges of particle energies. Different reasoning enters in the various ranges of rigidity R_L/l_c. Properly normalized, the results apply equally well to relativistic and non-relativistic particle transport, provided that the random magnetic field is isotropic with zero mean.

Appendix A
Relation between Diffusion Coefficients in Velocity Space and Position Space

We proceed using spatial and temporal variables divided into slow variables X and T, and fast variables ξ and τ, respectively. The slow and the fast variables can be written in terms of a small parameter ϵ as

$$T = \epsilon^2 t, \quad X = \epsilon x$$
$$\tau = t, \quad \xi = x \,.$$

The motivation for different time ordering when compared to the spatial ordering comes from the fact that, if we let ϵ be the ratio of scattering length scale to the transport length scale, then from the spatial diffusion equation a simple dimensional analysis shows that the ratio of scattering timescale to the

transport timescale should be of the order of ϵ^2 (see, e.g., Frisch 1995).

The derivatives can then be written as

$$\frac{\partial}{\partial t} = \frac{\partial}{\partial \tau} + \epsilon^2 \frac{\partial}{\partial T},$$
$$\nabla_x = \nabla_\xi + \epsilon \nabla_X.$$

Considering Equation (3) (Fokker–Plank equation), we seek a solution for the distribution function f with

$$f = f^{(0)} + \epsilon f^{(1)} + \epsilon^2 f^{(2)} + ..., \tag{47}$$

where each order of f can be expanded in terms of the spherical harmonics $Y_{lm}(\theta, \phi)$ (Equation (5)), which satisfy

$$v^2 \nabla_\perp^2 Y_{lm}(\theta, \phi) = [-l(l+1)] Y_{lm}(\theta, \phi). \tag{48}$$

The expansion in Equation (47) is inserted into Equation (4). With the help of Equations (5) and (48), we get separate equations for each of the different orders of f.

The $O(\epsilon^0)$ terms give

$$\frac{\partial f^{(0)}}{\partial \tau} + \boldsymbol{v} \cdot \nabla_\xi f^{(0)} = D_v \nabla_\perp^2 f^{(0)}. \tag{49}$$

Now we introduce an operator $\langle \cdots \rangle$, which is the spacetime average over the fast variables. Since all variables will be assumed to have finite variations in time and space, the averaging operator gives a zero result when operating on any quantity that may be written as a derivative with respect to fast variables. This is also known as the solvability condition so that we have a closed form of equations. Also, let $\langle f^{(q)} \rangle = F^{(q)}$.

Equation (49) averaged over the fast variables gives

$$D_v \nabla_\perp^2 F^{(0)} = 0, \tag{50}$$

which implies that $F^{(0)}$ is isotropic in $\boldsymbol{v}$.

Averaged over the fast variables, the $O(\epsilon^1)$ term is

$$\boldsymbol{v} \cdot \nabla_X F^{(0)} = D_v \nabla_\perp^2 F^{(1)}. \tag{51}$$

Without loss of generality, we may pick the direction of the gradient to be the z-direction. The left-hand side of Equation (51) has a projection only onto the Y_{10} term of the spherical harmonics. The right-hand side must also have a projection onto the Y_{10} term. With the help of Equations (5) and (48) in Equation (51), one finds

$$\boldsymbol{v} \cdot \nabla_X F^{(0)} = -2 \frac{D_v}{v^2} F^{(1)} \Rightarrow F^{(1)} = \frac{-v^2}{2D_v} \boldsymbol{v} \cdot \nabla_X F^{(0)}. \tag{52}$$

When averaged over the fast variables, the $O(\epsilon^2)$ term gives

$$\frac{\partial F^{(0)}}{\partial T} + \boldsymbol{v} \cdot \nabla_X F^{(1)} = D_v \nabla_\perp^2 F^{(2)}. \tag{53}$$

Substituting the relation between $F^{(1)}$ and $F^{(0)}$ from Equation (52) into Equation (53), one gets

$$\frac{\partial F^{(0)}}{\partial T} - \frac{v^2}{2D_v}(v_i v_j \nabla_{X_i} \nabla_{X_j}) F^{(0)} = D_v \nabla_\perp^2 F^{(2)}, \tag{54}$$

where a repeated index indicates summation. To study the diffusion of the bulk distribution, we consider the average over all directions. From Equation (48), we see that the right-hand

side of Equation (54) averages to zero. Using

$$[v_i v_j]_{\text{direction averaged}} = \frac{v^2}{3} \delta_{ij}, \tag{55}$$

we then obtain

$$\frac{\partial F^{(0)}}{\partial T} = \frac{v^4}{6D_v} \nabla_X^2 F^{(0)}. \tag{56}$$

This is a diffusion equation in configuration space with diffusion coefficient

$$\kappa = \frac{v^4}{6D_v}.$$

Appendix B
Angular Deflection of a Magnetic Field Line Over an Inertial Range of Turbulence

We examine the angular deflection of a field line over a separation l from the perspective of turbulence theory. The magnetic field vector and its associated field lines experience a change of direction due to the turbulence. If we initially start with no transverse component, then the transverse component at a separation l in the inertial range of turbulence can be estimated approximately for an ensemble of field lines by Kolmogorov's law.

Let $S_2^t(l)$ be the second-order transverse structure function with separation l. Kolmogorov's 2/3 law states that

$$S_2^t(l) = \delta b_l^2 = \langle [b_t(\boldsymbol{x}) - b_t(\boldsymbol{x}+l)]^2 \rangle \propto l^{2/3}.$$

If $S_2^t(l_c)$ is the second-order transverse structure function at a separation of a correlation length l_c, then one finds

$$\frac{\delta b_l^2}{\delta b_c^2} = \left(\frac{l}{l_c}\right)^{2/3}.$$

Initially, there is no transverse component and if approximately 2/3 of the energy is present in the transverse component at the correlation length, then

$$\delta b_l^2 \approx \frac{2}{3} \delta b^2 \left(\frac{l}{l_c}\right)^{2/3},$$

and

$$\frac{\delta b_l}{|\delta b|} \approx 0.8 \left(\frac{l}{l_c}\right)^{1/3}.$$

If θ is the angular deflection at the mean-free path of a particle λ, then

$$\sin \theta = \frac{\delta b_l}{|\delta b|} \approx 0.8 \left(\frac{\lambda}{l_c}\right)^{1/3}.$$

For $R_L/l_c = 0.01$, which is relevant for a low energy that is numerically attainable, our numerical results give $\lambda = 0.1\, l_c$, implying $\theta \approx 20^0$. At lower particle energy, the relevant angular deflection is still smaller. We neglect this deflection in the low-energy quasilinear theory presented in Section 5.

Appendix C
Non-relativistic Example

To provide a broader context, in Figure 3, we evaluate the theory for the case of non-relativistic particles or moderately
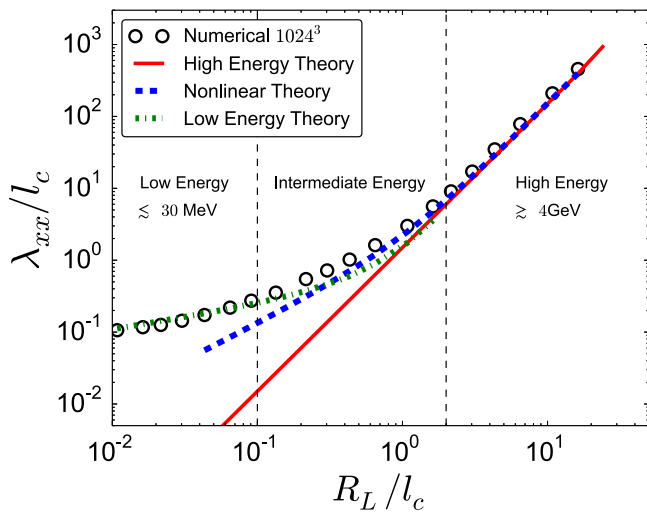
Figure 3. Theoretical vs. numerical results for non-relativistic or moderately relativistic charged particles in isotropic turbulence with zero mean field for parameters as listed in Appendix C. The circles represent the numerical results, the solid line represents the high-energy theory, the dashed line is the nonlinear theory and the dotted–dashed line is the theoretical estimate for low energies. The energy ranges are shown for protons and magnetic field parameters for interplanetary turbulence. The results also apply to any non-relativistic particles of a given R_L/l_c.

relativistic particles. For convenience, we adopt parameters that closely resemble interplanetary space in our solar system, except that here no mean magnetic field is included. For this example, the particles are non-relativistic at low energies with $R_L/l_c < 1$, but become moderately relativistic at higher energies. The correlation length is chosen to be $l_c = 0.01$ au and the root-mean-square magnetic field to be 5 nT (Burlaga et al. 2013). Then $R_L = l_c$ at 1.5 GeV. The theoretical mean-free paths depend only on rigidity, and the test particle simulation is in close agreement whether the particles are relativistic or non-relativistic.

It is well known that the interplanetary turbulent magnetic field is represented by an anisotropic spectral model in which the fluctuations are of the same order of magnitude as the mean field. Numerous realistic studies have also been performed and compared with observational results in the past (e.g., Tautz & Shalchi 2013), so our study with isotropic turbulence and no background field should be interpreted as simply a test case.

References

Q1

Aguilar, M., Ali Cavasonza, L., Ambrosi, G., et al. 2016, PhRvL, 117, 231102
Aloisio, R., & Berezinsky, V. 2004, ApJ, 612, 900

Batchelor, G. K. 1953, The Theory of Homogeneous Turbulence
Batchelor, G. K. 1969, PhFl, 12, II233
Bieber, J. W., & Matthaeus, W. H. 1997, ApJ, 485, 655
Bieber, J. W., Matthaeus, W. H., Shalchi, A., & Qin, G. 2004, GeoRL, 31, L10805
Bieber, J. W., Smith, C. W., & Matthaeus, W. H. 1988, ApJ, 334, 470
Blasi, P. 2013, A&ARv, 21, 70
Blasi, P., Burles, S., & Olinto, A. V. 1999, ApJL, 514, L79
Burlaga, L., Ness, N., & Stone, E. 2013, Sci, 341, 147
Caprioli, D. 2015, arXiv:1510.07042
Caprioli, D., & Spitkovsky, A. 2014, ApJ, 794, 47
Casse, F., Lemoine, M., & Pelletier, G. 2002, PhRvD, 65, 023002
Corrsin, S. 1959, in Advances in Geophysics, Atmospheric Diffusion and Air Pollution, Vol. 6, ed. F. Frenkel & P. Sheppard (New York: Academic), 161
de Marco, D., Blasi, P., & Stanev, T. 2007, JCAP, 2007, 027
Dupree, T. H. 1966, PhFl, 9, 1773
Dupree, T. H. 1967, PhFl, 10, 1049
Earl, J. A. 1974, ApJ, 193, 231
Fisk, L. A., Goldstein, M. L., Klimas, A. J., & Sandri, G. 1974, ApJ, 190, 417
Frisch, U. 1995, Turbulence. The Legacy of A. N. Kolmogorov
Ghilea, M. C., Ruffolo, D., Chuychai, P., et al. 2011, ApJ, 741, 16
Goldstein, M. L. 1976, ApJ, 204, 900
Gombosi, T., Cravens, T. E., Nagy, A. F., Brace, L. H., & Owens, A. J. 1979, GeoRL, 6, 349
Green, M. S. 1951, JChPh, 19, 1036
Harari, D., Mollerach, S., & Roulet, E. 2002, JHEP, 7, 006
Hasselmann, K., & Wibberenz, G. 1970, ApJ, 162, 1049
Hauff, T., Jenko, F., Shalchi, A., & Schlickeiser, R. 2010, ApJ, 711, 997
Jansson, R., & Farrar, G. R. 2012, ApJ, 757, 14
Jokipii, J. R. 1966, ApJ, 146, 480
Jokipii, J. R., & Parker, E. N. 1968, PhRvL, 21, 44
Jones, F. C., Kaiser, T. B., & Birmingham, T. J. 1973, Proc. ICRC, 2, 669
Karimabadi, H., Krauss-Varban, D., & Terasawa, T. 1992, JGR, 97, 13
Kronberg, P. P. 1994, RPPh, 57, 325
Kubo, R. 1957, JPSJ, 12, 570
Mace, R. L., Dalena, S., & Matthaeus, W. H. 2012, PhPl, 19, 032309
Matthaeus, W. H., Qin, G., Bieber, J. W., & Zank, G. P. 2003, ApJL, 590, L53
Minter, A. H., & Spangler, S. R. 1996, ApJ, 458, 194
Obermeier, A., Boyle, P., Hörandel, J., & Müller, D. 2012, ApJ, 752, 69
Owens, A. J. 1974, ApJ, 191, 235
Parizot, E. 2004, NuPhS, 136, 169
Plotnikov, I., Pelletier, G., & Lemoine, M. 2011, A&A, 532, A68
Qin, G., Matthaeus, W. H., & Bieber, J. W. 2002, GeoRL, 29, 7
Qin, G., & Shalchi, A. , 2009, ApJ, 707, 61
Reville, B., O'Sullivan, S., Duffy, P., & Kirk, J. G. 2008, MNRAS, 386, 509
Ruffolo, D., Pianpanit, T., Matthaeus, W. H., & Chuychai, P. 2012, ApJL, 747, L34
Ruzmaikin, A. A., Sokoloff, D., & Shukurov, A. M. 2013, Magnetic Fields of Galaxies, Vol. 133 (Springer Science & Business Media)
Shalchi, A. 2006, A&A, 453, L43
Shalchi, A. 2009, Nonlinear Cosmic Ray Diffusion Theories
Shalchi, A. 2010, ApJL, 720, L127
Shalchi, A., Bieber, J. W., Matthaeus, W. H., & Qin, G. 2004, ApJ, 616, 617
Snodin, A. P., Shukurov, A., Sarson, G. R., Bushby, P. J., & Rodrigues, L. F. S. 2016, MNRAS, 457, 3975
Sonsrettee, W., Subedi, P., Ruffolo, D., et al. 2015, ApJ, 798, 59
Tautz, R. C., & Shalchi, A. 2013, JGRA, 118, 642
Tautz, R. C., Shalchi, A., & Schlickeiser, R. 2008, ApJL, 685, L165
Taylor, G. I. 1922, Proc. London Math. Soc, 20, 196

Q2

Q3

10